The Astrophysical Journal, 817:100 (15pp), 2016 February 1 doi:10.3847/0004-637X/817/2/100

THE REFLARES AND OUTBURST EVOLUTION IN THE ACCRETING MILLISECOND PULSAR SAX J1808.4–3658: A DISK TRUNCATED NEAR CO-ROTATION?

A. Patruno[1,2], D. Maitra[3], P. A. Curran[4], C. D'Angelo[1], J. K. Fridriksson[5], D. M. Russell[6], M. Middleton[7], and R. Wijnands[5]

[1] Leiden Observatory, Leiden University, Neils Bohrweg 2, 2333 CA, Leiden, The Netherlands
[2] ASTRON, the Netherlands Institute for Radio Astronomy, Postbus 2, 7900 AA, Dwingeloo, The Netherlands
[3] Department of Physics & Astronomy, Wheaton College, Norton, MA 02766, USA
[4] International Centre for Radio Astronomy Research—Curtin University, GPO Box U1987, Perth, WA 6845, Australia
[5] Anton Pannekoek Institute, University of Amsterdam, Science Park 904, 1098 XH, Amsterdam, The Netherlands
[6] New York University Abu Dhabi, P.O. Box 129188, Abu Dhabi, United Arab Emirates
[7] Institute of Astronomy, Madingley Rd, Cambridge CB3 0HA, UK
Received 2015 April 17; accepted 2015 November 12; published 2016 January 26

ABSTRACT

The accreting millisecond X-ray pulsar SAX J1808.4–3658 shows peculiar low luminosity states known as "reflares" after the end of the main outburst. During this phase the X-ray luminosity of the source varies by up to three orders of magnitude in less than 1–2 days. The lowest X-ray luminosity observed reaches a value of $\sim 10^{32}$ erg s^{-1}, only a factor of a few brighter than its typical quiescent level. We investigate the 2008 and 2005 reflaring state of SAX J1808.4–3658 to determine whether there is any evidence for a change in the accretion flow with respect to the main outburst. We perform a multiwavelength photometric and spectral study of the 2005 and 2008 reflares with data collected during an observational campaign covering the near-infrared, optical, ultra-violet and X-ray band. We find that the NIR/optical/UV emission, expected to come from the outer accretion disk, shows variations in luminosity over an order of magnitude. The corresponding X-ray luminosity variations are instead much deeper, spanning about 2–3 orders of magnitude. The X-ray spectral state observed during the reflares does not change substantially with X-ray luminosity, indicating a rather stable configuration of the accretion flow. We investigate the most likely configuration of the innermost regions of the accretion flow and we infer an accretion disk truncated at or near the co-rotation radius. We interpret these findings as due to either a strong outflow (due to a propeller effect) or a trapped disk (with limited/no outflow) in the inner regions of the accretion flow.

Key words: accretion, accretion disks – pulsars: general – pulsars: individual (SAX J1808.43658) – stars: neutron – X-rays: binaries

1. INTRODUCTION

SAX J1808.4–3658 is a binary X-ray transient discovered in 1996 (in't Zand et al. 1998) and located at a distance of 2.5–3.5 kpc (in't Zand et al. 1998; Galloway & Cumming 2006). The binary is composed of a 401 Hz accreting millisecond X-ray pulsar (Wijnands & van der Klis 1998; see Patruno & Watts 2012 for a review) and a semi-degenerate companion of mass $\sim 0.07\ M_{\odot}$ (Bildsten & Chakrabarty 2001; Deloye et al. 2008). The system has an orbital period of 2 hr (Chakrabarty & Morgan 1998) and the accreting neutron star has an inferred magnetic field of $\sim 10^8$ G (Psaltis & Chakrabarty 1999; Di Salvo & Burderi 2003; Hartman et al. 2008; Patruno et al. 2012).

The seven outbursts of SAX J1808.4−3658 observed so far (in 1996, 1998, 2000, 2002, 2005, 2008 and 2011) have a recurrence time of ∼2–3.5 years and show a main outburst with a fast rise followed by a slow decay and a rapid drop (see e.g., Figure 2 in Hartman et al. 2008). After the end of the main outburst, lasting for approximately one month, there is a long "reflaring" tail[8] at low X-ray luminosities (10^{32-35} erg s^{-1}) lasting for several tens of days (see e.g., Wijnands et al. 2001; Revnivtsev 2003; Wijnands 2003; Hartman et al. 2008; Patruno et al. 2009b, 2012). Such reflares manifest themselves as smooth variations in luminosity that appear cyclically every few days. Furthermore, on one occasion (during the 2005 outburst) a very low luminosity phase has been reported (Campana et al. 2008). This later phase was called "metastable" since it occurred at an X-ray luminosity of 1.5–5 $\times$ 10^{32} erg s^{-1} (0.5–10 keV), a value compatible with the lowest X-ray luminosities reached during the reflares (Wijnands et al. 2001; Patruno et al. 2009b) and only a factor of a few brighter than the typical quiescent luminosities. It is currently unclear whether this phase is really different from the reflaring phase or whether the sparse *Swift* monitoring observed only the low luminosity phase of the reflares themselves. After this possible metastable state the source turned back to quiescence, when the 0.5–10 keV X-ray luminosity reached a value of 5 $\times$ 10^{31} erg s^{-1} (Campana & Stella 2004; Heinke et al. 2009).

The typical variation on luminosity observed during the reflares of SAX J1808.4−3658 spans approximately one order of magnitude (10^{34}–10^{35} erg s^{-1}, see e.g., Patruno et al. 2009b). However, in at least three occasions (during the 2000, 2005 and 2008 outbursts) the reflares showed a dramatic decrease in luminosity with an excursion of three orders of magnitude on a timescale shorter than ∼2 days (Wijnands 2003; Campana et al. 2008; Patruno et al. 2009b). The faintest luminosities reach a value of ∼3 $\times$ 10^{32} erg s^{-1} (for a distance[9] of 3.5 kpc) which

[8] The 1998 and 2011 outbursts are poorly constrained as the observations stopped close to the end of the main outburst, see Patruno et al. (2012, 2009b).

[9] Wijnands (2003) reports a luminosity of 1.7 $\times$ 10^{32} erg s^{-1} for a distance of 2.5 kpc. Rescaling to 3.5 kpc—the distance adopted in this work—gives 3.3 $\times$ 10^{32} erg s^{-1}.

is slightly higher than the typical quiescent one (5–8 $\times$ 10^{31} erg s^{-1} at 3.5 kpc, Campana & Stella 2004; Heinke et al. 2009). Such low luminosities were observed thanks to the sensitivity of the *XMM-Newton* and *Swift* observatories and we cannot exclude that something similar might have happened in all the other outbursts recorded so far (which were observed, in X-rays, exclusively by the *Rossi X-ray Timing Explorer*, *RXTE*).

Reflares (also known in the literature as "rebrightenings," "echo-outbursts," "mini-outbursts" and "flaring-tail") have been observed in a number of different systems, including dwarf novae (WZ Sge, Patterson et al. 2002; EG Cnc, Osaki et al. 2001; ER UMA Robertson et al. 1995; Patterson et al. 2013, AL Com Howell et al. 1996, UZ Boo, Kuulkers et al. 1996; BK Lyn Patterson et al. 2013), neutron stars (e.g., KS 1731-260, Šimon 2010, SAX J1750.8–2900 Allen et al. 2015 and possibly IGR J00291+5934, Lewis et al. 2010) and black hole low-mass X-ray binaries (LMXBs) (e.g., XTE J1650–500, Tomsick et al. 2004; GRO J0422+32, Kuulkers et al. 1996; GRS 1009–45, Bailyn & Orosz 1995; XTE J1859+226, Zurita et al. 2002; 4U 1543–47, Li et al. 1976). The ubiquity of the phenomenon among different types of accreting compact objects suggests that reflares are related to specific properties of the accretion disk itself rather than properties of the compact object.

Reflares are not a feature that can be easily justified within the *disk instability model* (DIM; see the extended reviews of Smak 1984; Menou et al. 2000; Dubus et al. 2001; Lasota 2001; Kotko et al. 2012). Reflares are observed in numerical DIM simulations and they are created by back and forth propagation of cold and hot waves that re-combine and ionize the accretion disk cyclically. However, these reflares are considered a "deficiency" of the DIM model rather than a feature, since they cannot reproduce almost any of the properties observed in dwarf novae and soft X-ray transients (Dubus et al. 2001; Lasota 2001). Furthermore reflares require a large reservoir of matter to be still in the disk once the main outburst is over, whereas the DIM predicts that the accretion disk should be almost devoid of matter toward the end of an outburst (Dubus et al. 2001; Arai et al. 2009).

An interesting aspect of the reflares seen in SAX J1808.4−3658 is that the physical conditions in the inner regions of the accretion disk are strongly affected by the presence of its magnetosphere, since accretion-powered pulsations are observed throughout the outbursts, including large portions of the reflares in 2000, 2002, 2005 and 2008 (at least at luminosities $\simeq 10^{35}$ erg s^{-1}, where *RXTE* has sufficient sensitivity to detect them, see Hartman et al. 2008, 2009).

During the 2008 outburst, SAX J1808.4−3658 had been monitored with a multi-wavelength campaign that involved the *RXTE*, the *Swift* X-Ray Telescope (XRT) and Optical and Ultra-Violet Telescope (UVOT) and by ground-based optical/NIR observations in the *I* and *H* bands taken with the 1.3 m *SMARTS* telescope. The fact that SAX J1808.4−3658 is an accreting millisecond pulsar with a dynamically important magnetosphere plus the unique multiwavelength coverage is key to simultaneously probe different regions of the accretion disk/flow. In this paper we report the results of the multi-wavelength campaign on the 2008 outburst with a particular focus on its reflares. We also analyze the *Swift*/UVOT and XRT data collected during the 2005 reflaring phase and "metastable" state and compare them with the 2008 outburst and with the 2005 analysis already reported in Campana et al. (2008). We investigate whether during the reflaring phase our observations show any evidence for anomalies in the behavior of the accretion flow and whether there is any evidence in support of any of the current models that try to explain the reflares phenomenon.

2. OBSERVATIONS

We used data collected with four different detectors/telescopes: the optical/NIR ANDICAM on the 1.3 m *SMARTS* telescope (operated by the *SMARTS* Consortium; Subasavage et al. 2010), the *Swift*/UVOT (Roming et al. 2005), the *Swift*/XRT (0.3–10 keV; Burrows et al. 2005) and the Proportional Counter Array (PCA) aboard *RXTE* (2–60 keV; Jahoda et al. 2006). In the following we describe the data reduction procedure for each waveband.

2.1. X-Ray Data

We analyzed 20 targeted *Swift* observations taken between 2008 September 24 and November 8 and 23 taken between 2005 June 17 and October 28 (see Table 1). Ten observations of 2008 and six of 2005 were taken during the main outburst, whereas the remaining monitored the reflaring phase. The XRT was operated in either photon-counting (PC) mode (2.5073-s time resolution) or in window-timing (WT) mode (1.7675-ms time resolution).

We extracted *Swift* count rates, spectra, and spectral response files for each individual ObsID using the online *Swift*/XRT data products generator[10] (Evans et al. 2007, 2009, 2014). The spectra were extracted (and fitted) in the 0.3–10 keV band using the default event grades (0–12 for PC mode and 0–2 for WT mode). The spectra were grouped with the GRPPHA task in HEASOFT (ver. 6.16) and fitted with XSPEC (ver. 12.8.2). Spectra containing $\gtrsim$150 counts were in general grouped to a minimum of 20 counts per bin and fitted with the χ^2 statistic, whereas spectra with fewer counts were grouped to a minimum of 1 count per bin and fitted with the W statistic (a modified version of the C statistic that allows background to be taken into account). For a few spectra with the largest number of counts we used a higher grouping minimum than 20 to avoid oversampling the spectral resolution of the detector by a large factor. Spectra with $\lesssim$15 counts were not fitted; instead the count rates were converted to fluxes assuming an absorbed power-law model. For ObsIDs where both PC and WT mode data exist we fitted spectra from both modes simultaneously (with all parameters tied) if the numbers of counts in the spectra were of the same order of magnitude, but otherwise only used data from one of the two modes (which was usually the case). We also calculated a hardness ratio for each ObsID based on the PC mode data only (where available); this was defined as the net counts in the 2–10 keV band divided by those in the 0.3–2 keV band.

Most of the data recorded in 2005 and 2008 by *RXTE* was already presented in Patruno et al. (2009b, 2012) and Hartman et al. (2009) and we refer to those works for in-depth details. Here we report a summary of that data analysis which is relevant for the results presented in this paper. For the *RXTE* data, we extracted the 2–16 keV energy band flux from the Standard2 mode data (16-s time resolution) collected by the PCA instrument during the 2005 and 2008 outbursts. The

[10] www.swift.ac.uk/user_objects/

Table 1
Observations of SAX J1808.4−3658 from 2005 to 2008

Year	Instrument	Program IDs	Obs-IDs	Data Range [MJD]
2005	*RXTE*/PCA	91418, 91056	91056-01-*, 91418-*-*-*	53522.8 to 53581.4
2008	*RXTE*/PCA	93027	93027-*-*-*	54731.9 to 54775.2
2005	*Swift*/XRT (PC)–*Swift*/UVOT (*v*)	30034, 30075	30034001–3, 30034005–6, 300340010–25 30075001, 30075020	53538.0 to 53671.1
2008	*Swift*/XRT (PC/WT)–*Swift*/UVOT (*v*, *b*, *u*, *w1*, *m2*, *w2*)	30034, 32582	30034026 to 30034044, 325827000	54733.8 to 54778.1
2008	*SMARTS*/CTIO-1.3 m (H, I)	N/A	N/A	54732.1 to 54781.0

background counts were calculated with the FTOOL `pca-backest` and were subtracted from the light curve along with dead-time corrections. The energy-channel conversion was done by using the `pca_e2c_e05v04` table provided by the *RXTE* team.

2.2. Space-borne UV/Optical Observations

The *Swift*/UVOT operated in imaging mode during all observations. Most of the observations (during the 2008 outburst) were taken with six filters (*v*, *b*, *u*, *w1*, *m2* and *w2*) wheres the last four exposures used the *u* filter only. The 2005 reflare were always observed with the *v* filter. We extracted the source photons from a circular region with a radius of 2.5 arcsec. The background was extracted from a circular region with radius of 10 arcsec far from bright sources. Before proceeding further, we manually inspected all UVOT images and found that some snapshots were affected by poor tracking. In particular some snapshots within the sequences corresponding to ObsIDs 30034036, 37 and 38 were affected and we only used those snapshots that were unaffected. Since the data was taken in image mode, bad snapshots themselves could not be corrected. We used the tool `uvotimsum` to add all UVOT exposures (snapshots) present in each FITS file into a single high signal-to-noise image and `uvotsource` to determine the optical/UV magnitudes using the Vega system (Poole et al. 2008). We then proceeded to de-redden the magnitudes by choosing a value for the neutral hydrogen absorption column of $N_{\rm H} = (1.4 \pm 0.2) \times 10^{21}\,{\rm cm}^{-2}$ (Patruno et al. 2009a). We used the relation (Güver & Özel 2009):

$$N_{\rm H} = (6.86 \pm 0.27) \times 10^{21} E(B-V) \quad (1)$$

to obtain $E(B-V) = 0.204 \pm 0.030$. The reddening for the six different filters is calculated according to Pei (1992) (see Table 2).

2.3. Ground-based Optical and Near-infrared Observations

The ground-based NIR (*I* and *H*-band) observations were made using the 1.3 m *SMARTS* telescope at the Cerro Tololo Inter-American Observatory (CTIO) in Chile. SAX J1808.4−3658 was observed with a roughly daily cadence (weather permitting) between 2008 September 22 and November 11. The *I*-band data were analyzed with the standard IRAF optical data reduction pipelines (Buxton et al. 2012) whereas for the NIR data multiple dithered frames were taken and then flat-fielded, sky subtracted, aligned, and average-combined using an in-house IRAF script. Three stars nearby SAX J1808.4−3658 and within the *SMARTS* field of view (FOV) were used as references and their average magnitudes were used as a basis for differential photometry with respect to SAX J1808.4−3658.

Table 2
Reddening Coefficient for Each of the Eight Optical/UV Filters on UVOT and *SMARTS* ($E(B-V) = 0.204 \pm 0.030$)

Filter	Reddening ($A_\lambda \pm \sigma_\lambda$)
H	0.11 ± 0.02
I	0.37 ± 0.06
v	0.62 ± 0.09
b	0.79 ± 0.12
u	1.00 ± 0.15
w1	1.38 ± 0.20
m2	1.96 ± 0.29
w2	1.64 ± 0.24

The *H*-band magnitudes of these reference stars were taken from the 2MASS point source catalog. For *I*-band we used the reference stars and their magnitudes from Greenhill et al. (2006), and compared these with the instrumental magnitudes obtained from *SMARTS* frames. We used the following zero-point fluxes to convert from magnitude to flux-density: $I_0 = 2416$ Jy (Bessell et al. 1998), and $H_0 = 980$ Jy (Frogel et al. 1978; Elias et al. 1982). We also de-reddened the magnitudes following the same procedure outlined above (see Table 2).

2.4. Contamination from Field Stars and Emission Lines

Since the point-spread-function of the UVOT telescope is rather poor (2.5 arcsec at 350 nm) and the field of SAX J1808.4−3658 is crowded we need to evaluate the amount of contaminating light from nearby stars that fall within our circular aperture extraction region. In our images the point-spread-function (which, in the absence of atmospheric effects, is given by a combination of pixel size and telescope optics) covers about 5 pixels (0.″5/pixel). By comparing the UVOT FOV of SAX J1808.4−3658 with Figure 2 in Wang et al. (2009) we found that part of the light emitted by a rather bright star leaks into the extraction region of SAX J1808.4−3658 (see Figure 1).

To verify how much the contamination is affecting our measurements we first selected three observations: one taken in 2005 (ObsID 30034018), one in 2008 (ObsID 30034040) and one during quiescence in 2014 August (ObsID 30034062). We chose the 2005 observation because the high signal-to-noise of the image allows a precise determination of the centroid of the contaminating object. The observation taken in 2008 is used to cover all six UVOT filters whereas the 2014 one is used to measure the UV flux during quiescence. We find that the contaminating object has the following magnitudes: $\sim$19.1 in *v*, $>$19.45 in *b*, $\sim$19.8 in *u* and $>$21 in *w1*. Since the minimum magnitude detected (for the extraction region centered around

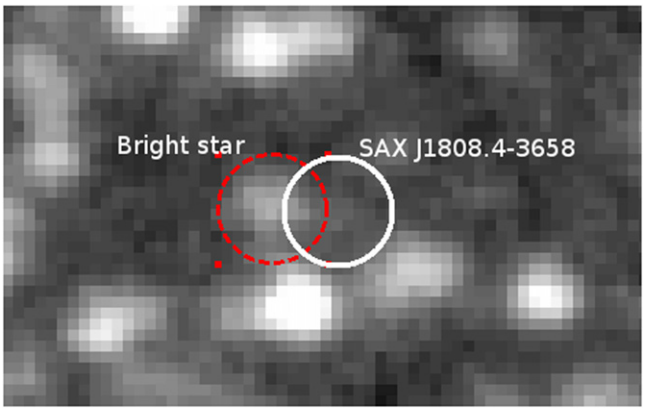

Figure 1. UVOT image of the FOV around SAX J1808.4–3658 taken with the *v* filter taken around MJD 53627.17 (ObsID 30034018, 2005 September 14). The dashed red circle highlights the 2.″5 region around a bright star whose light "leaks" into the extraction region used for SAX J1808.4−3658 (white circle).

SAX J1808.4−3658) is: ∼20 in *v*, 19.4 in *b*, ∼18.7 in *u* and 19.3 in *w1* we can confidently exclude that the contaminating source has an important effect in any but the *v* band.

A final point to consider is the possibility that the UV fluxes are contaminated by emission lines and therefore are not good tracers of the continuum emission. UV spectra of X-ray binaries can generally be well fitted with continuum models, with emission lines like Mg II sometimes visible, but they usually produce a small amount of flux compared to the continuum in the UV (Hynes et al. 1998, 2006; Hynes & Haswell 1999; Bayless et al. 2010). Small irregularities in the UV spectral energy distribution could therefore be due to the presence of prominent emission lines, but UV spectroscopy of X-ray binaries has shown that these usually make only a small-to-negligible difference to the continuum, and hence broadband UV filter fluxes.

3. RESULTS

3.1. The Multi-wavelength Light Curve

The multi-wavelength light curve of the 2008 outburst is shown in Figure 2. The reflares are observed at all wavelengths (with the exception of the first reflare, not monitored by *Swift*) with a typical cadence of about one observation every 2 days for *Swift*/XRT and UVOT, every 1–2 days in NIR with *SMARTS* and multiple observations per day with *RXTE*/PCA. The main outburst is fully covered with a high cadence monitoring with *RXTE* and observed by *SMARTS* for only two days close to the peak of the outburst and by *Swift* for 10 consecutive days during the slow decay.

The first *Swift*/XRT reflare observation is a non-detection and corresponds to an upper limit (95% confidence level) of less than ∼20 times the value detected in quiescence ($L_q \simeq 5$–8×10^{31} erg s^{-1}, Campana & Stella 2004; Heinke et al. 2007, 2009). The timescale of the reflares is about 7–12 days, which is substantially longer than the fast decay timescale (∼3 days; for a detailed discussion of the slow/fast decay in SAX J1808.4−3658 see Hartman et al. 2008). By comparing the behavior of the *I* and *H* magnitudes with that of the X-rays it appears that the NIR luminosity is higher than what would be expected when extrapolating the behavior seen during the slow decay. Indeed the two NIR observations occurring right after the beginning of the fast decay have an *H* and *I* magnitude higher than what would correspond to the X-ray flux detected on the closest dates (see Figure 2). Therefore it is possible that reflares start *earlier* in NIR by at least 1.5 days. The beginning of the other two reflares is ill constrained since the sampling is not sufficiently dense in X-rays, but the observations are still compatible with an earlier response of the NIR.

The last detection of the reflaring phase occurs at MJD 54781 (*I* band) at a level compatible with what observed during the reflares minima. The source is not detected in the *H* band and no observations are performed during that time with the *Swift*/XRT and UVOT. It is therefore difficult to determine whether we have detected the beginning of a new reflare, the beginning of a "metastable" state similar to what reported by Campana et al. (2008) at the end of the 2005 outburst or something different. The *I* band magnitude detected at MJD 54781 is ∼2.5 mag. brighter than the quiescent *I* detected in the 1998 outburst (Campana et al. 2004) so that we can at least confidently conclude that some activity is still ongoing at the time of the observation. We also inspected the publicly available light curves taken with the All Sky Monitor aboard *RXTE* and the Burst Alert Telescope on *Swift*. We found a few data points close to the 3σ detection level, but none of them is statistically significant given the number of data points (trials) considered (i.e., 3248 data points). The constraints on the luminosity placed by these two instruments are not particularly strong since they correspond to luminosities of the order of a few times 10^{35} erg s^{-1}, which are values reached only during the brightest portions of the reflares.

The *v* band magnitudes (not de-reddened) of the 2005 outburst are shown in Figure 3 along with the 2–16 keV and 0.3–10 keV X-ray flux. Several observations (highlighted with blue circles in the figure) show a lack of correlation between the *v* magnitudes and the X-ray flux.

3.2. X-Ray–Optical/UV/NIR Correlation

By looking at Figure 2 we can see how the X-ray luminosity variations co-vary with the the NIR, optical and UV luminosity. However, the excursion seen in X-rays spans at least 2 orders of magnitude, whereas the NIR/optical/UV changes by approximately 3 mag, which translates into a flux variation of a factor ≈10–20. Therefore, we do not expect a steep correlation between X-ray flux and NIR/optical/UV magnitudes. Furthermore, on several occasions the X-rays and NIR/optical/UV do not correlate and seem to be varying independently (see e.g., circled points in Figure 3 and data points around MJD 54760 in Figure 2 and discussion in Section 4.1.1).

In this section we estimate the correlation between these quantities. Since the variations in luminosity can happen on very short timescales, we decided to consider only the optical, UV and X-ray emission recorded with the UVOT and the XRT and to exclude the ground-based optical/NIR data since they are not taken simultaneously with the X-ray data, but have a typical offsets of ∼0.5–1 day. The advantage of using the UVOT and XRT data is that these telescopes operate strictly simultaneously (although the exposure times are not necessarily the same). One exception is represented by one ground-based *I* and *H* band observation from MJD 54758 taken within 1 hr of a *Swift* pointing. In this case we decided to consider the ground-based data as (quasi)simultaneous.

In Figure 4 we plot the de-reddened optical to X-ray (unabsorbed) luminosity relation for the *Swift* observations of

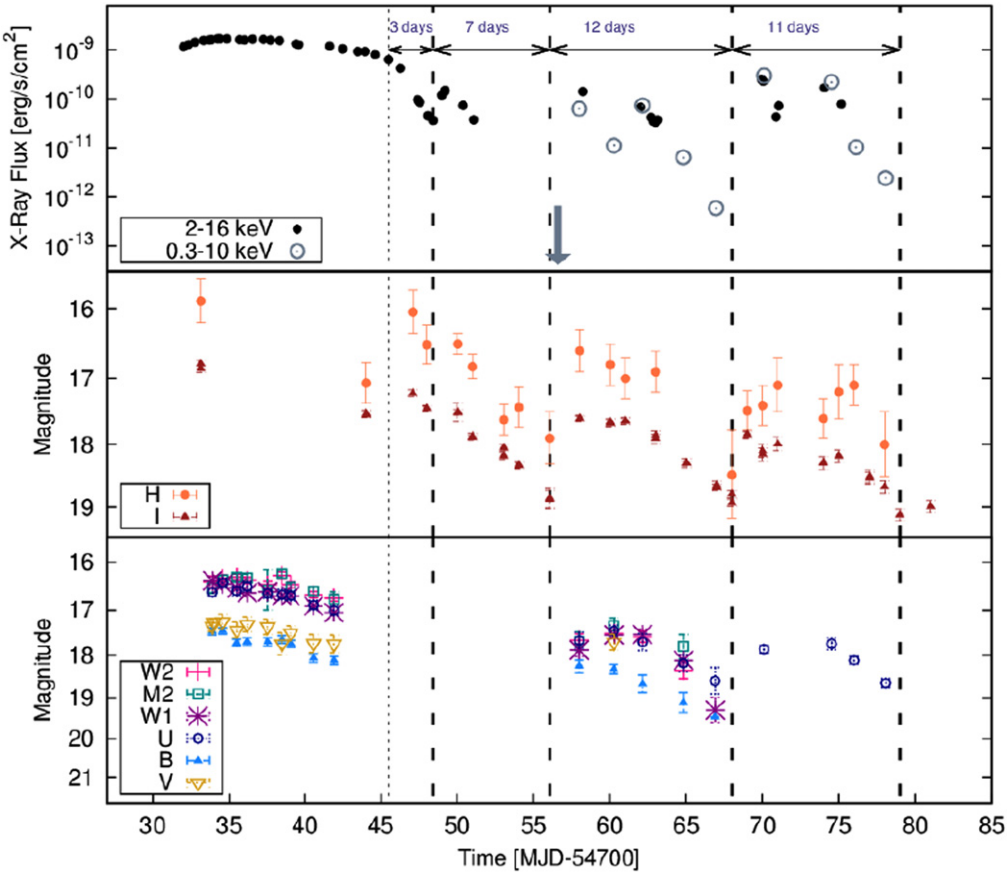

Figure 2. Multi-wavelength light curve of the 2008 outburst. The X-ray flux and the NIR/optical/UV magnitudes are *not* corrected for absorption/reddening but refer to the observed values. Top panel: the observed X-ray light curve recorded with *RXTE* (2–16 keV; filled black circles) and *Swift*/XRT (0.3–10 keV; open gray circles). The vertical dotted line marks the approximate beginning of the rapid drop. The dashed vertical lines identify the most likely limits for the start and end of each reflare. The down-arrow marks a non-detection. Middle panel: optical/NIR observations with the *H* (central $\lambda = 16500$ Å) and *I* (central $\lambda = 7980$ Å) filters. Bottom panel: optical and UV observations carried with the UVOT (for the central λ of each filter we refer to Table 3). The non-detections are not reported.

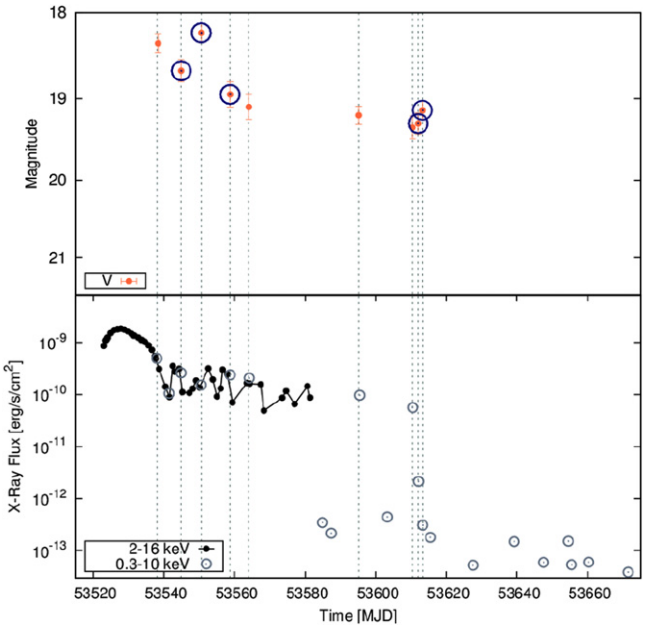

Figure 3. Top Panel: *v* band light curve (*Swift*/UVOT) of SAX J1808.4–3658 during the 2005 outburst reflare. The magnitudes are *not* de-reddened. Bottom Panel: 2005 outburst X-ray light curve observed with *RXTE*/PCA (2–16 keV) and *Swift*/XRT (0.3–10 keV).

the 2005–2008 outbursts plus additional data referring to other neutron star LMXBs where these two quantities are measured (and found to be correlated, see Russell et al. 2006, 2007 for details).[11] We used the 2–10 keV energy band rather than the 0.3–10 keV in order to match the analysis of Russell et al. (2006) done for the other neutron star LMXBs used in Figure 4. Some of the 2008 data lie slightly above the correlation with a slope that is somewhat flatter than recorded for other neutron star LMXBs. The offset between our data points and the other archival data is not surprising since the latter points are taken with the *BVRI* filters, whereas our data points are mainly composed of *u* and UV data and only very few data points are taken with the *I*, *b* and *v* filters. Indeed such an effect is not observed in 2005 when the UVOT used only the *v* filter. Similar (instrumental) offsets have been observed already in other sources (see e.g., van der Horst et al. 2013).

The flatter slope instead needs an explanation and to quantify this, we first fitted a simple power law relation $F_{\rm UV/Opt} = k\, F_{\rm X}^{\beta}$, where $F_{\rm UV/Opt}$ is the flux in one of the optical/UV bands, $F_{\rm X}$ is the 2–10 keV X-ray flux, β is the slope and k is a constant of proportionality. Russell et al. (2006, 2007) estimated the coefficient β for neutron stars (assuming a radiatively efficient accretion flow, $L_{\rm X} \propto \dot{M}$) and black holes (with a radiatively

[11] The correlation between optical and X-ray flux found by Russell et al. (2006, 2007) are empirical rather than theoretical.

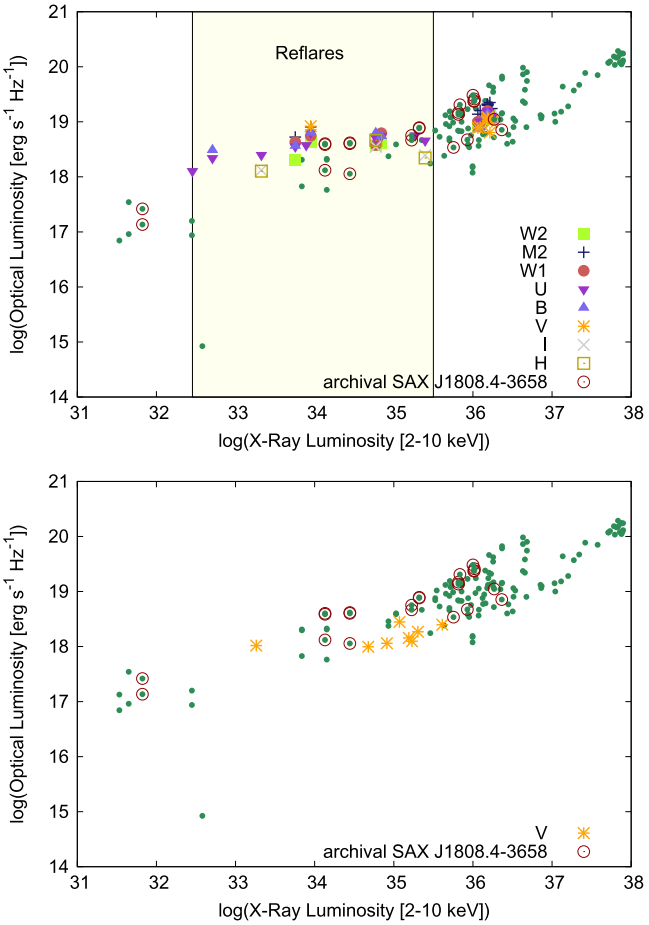

Figure 4. Top Panel: NIR–optical–UV/X-ray correlation diagram. The green points show the correlation for several different neutron star LMXBs (Russell et al. 2006, 2007). A few points (circled in red) refer to (archival) SAX J1808.4–3658 data taken during quiescence or during its 1998 outburst. The 2008 *Swift* observations reported in this paper are shown with different symbols/color depending on the specific filter used. Bottom Panel: same as top panel but for the 2005 outburst.

Table 3
Correlation Coefficient between the UV/Optical and X-Ray Fluxes

UVOT/Band	$\lambda_{central}$ (Å)	β
w2	1928	0.28 ± 0.05
m2	2246	0.24 ± 0.06
w1	2600	0.22 ± 0.05
u	3465	0.23 ± 0.05
b	4392	0.16 ± 0.04
v_{2008}	5468	0.03 ± 0.05
v_{2005}	5468	0.05 ± 0.21
I	7980	0.11 ± 0.13

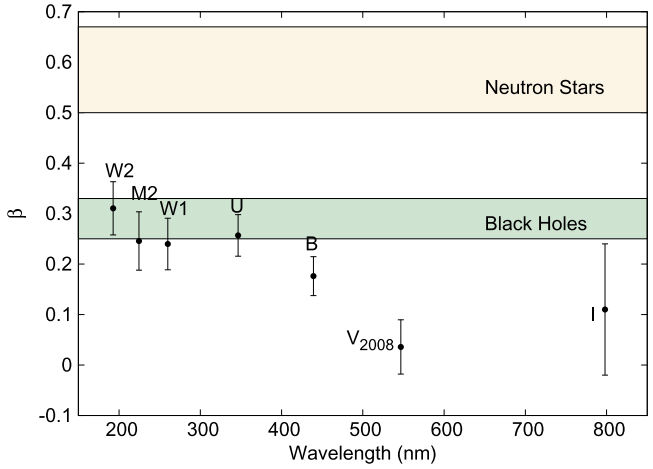

Figure 5. Correlation coefficient β calculated for seven different optical/UV bands for the 2008 outburst. The β value for the *v* band of the 2005 outburst is unconstrained and is not displayed. The two colored bands indicate the theoretical β values expected for black hole LMXBs (in green) and neutron stars LMXBs (in yellow). The difference in the location of the two bands reflects the different accretion efficiency ($\propto \dot{M}$ for neutron stars and $\propto \dot{M}^2$ for black holes). Most data points of SAX J1808.4−3658 fall within the black holes band. The value of β is also consistent with increasing toward shorter wavelengths, a typical behavior expected in viscous heated accretion discs rather than irradiated ones.

inefficient accretion flow (RIAF), $L_X \propto \dot{M}^2$). Since we are using optical/UV wavebands, the expected range of β for a viscously heated disk is $0.5 < \beta < 0.67$ for neutron stars and $0.25 < \beta < 0.33$ for black holes (Russell et al. 2006). In Table 3 and Figure 5 we report the results of our fit.

All bands, with the exception of the *v* and *I* bands, show a flux that is clearly correlated with the X-ray flux. However, the value of the correlation coefficient β falls within the 0.15–0.25 range (again, excluding the *v* and *I* bands). These values are significantly smaller than those seen in other neutron star LMXBs (e.g., Maitra & Bailyn 2008; Armas Padilla et al. 2013). The values of β also increase with decreasing wavelength, as found in viscously heated disks (see e.g., Russell et al. 2006; Armas Padilla et al. 2013). For irradiated disks or for jet-dominated optical emission, the expected values of β are also higher than observed.

3.3. Rayleigh–Jeans Limit

The shallow slope of the F_X versus $F_{opt/UV}$ relation could also be explained if the optical/UV emission falls in the Rayleigh–Jeans (RJ) limit of the multicolor-blackbody accretion disk spectrum. To test this hypothesis we selected five observations with the source detected in at least four UVOT filters. Of these observations, four were taken during the reflares whereas a "control" group was chosen from the main outburst. We then fitted $F_{opt/UV} \propto \nu^{\alpha}$ and checked whether $\alpha \approx 2$ as expected in the RJ limit. In one observation we included also the ground-based optical/NIR observations since these data were recorded within 1 hr from the UVOT and XRT data. We also fitted a correlation with α forced to be equal to 2 as expected in the RJ limit. In Table 4 and Figure 6 we report the observation selected and the results of our fit.

None of the observations show an α compatible with being 2. Three out of five observations cannot be fitted with a simple power-law relation (i.e., unacceptable χ^2). However, by looking at the panel "(a)" of Figure 6, which refers to the observation taken during the main outburst, it appears that we might still be in the RJ limit for all optical/UV filters if the location of the data points is somehow affected by unaccounted systematics (see discussion below). Panels "(d)" and "(e)" are compatible with the RJ limit if the peak of the blackbody emission falls around the *m2* and *w2* band. In the panel "(b)" and "(c)" there seems to be stronger deviations from the RJ limit, with α being closer to values of 0–1. These two observations might be explained if the blackbody peak toward lower energies. However, the optical/UV luminosity is slightly

Table 4
Observations Used to Test for the Rayleigh–Jeans Limit

Panel	Phase	ObsId	MJD	Filters	α	χ^2/dof
(a)	Main Outburst	30034031	54738.4	*v, b, u, w1, m2, w2*	1.4 ± 0.3	37.7/4
(b)	Reflare	30034036	54758.0	*H, I, b, u, w1, m2, w2*	0.93 ± 0.11	30.5/5
(c)	Reflare	30034037	54760.3	*v, b, u, w1, m2, w2*	0.48 ± 0.18	7.37/4
(d)	Reflare	30034038	54762.1	*b, u, w1, w2*	0.58 ± 0.28	2.9/2
(e)	Reflare	30034039	54764.8	*b, u, w1, m2, w2*	0.32 ± 0.50	10.80/3

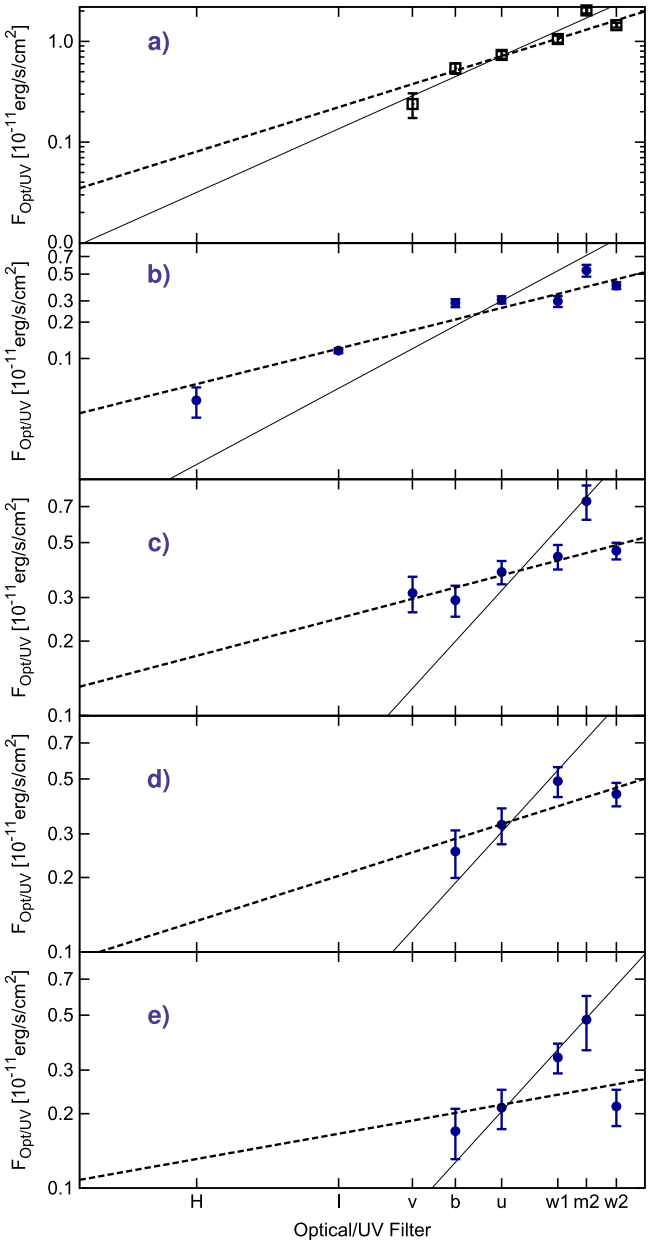

Figure 6. Optical/UV flux vs. UVOT filter central frequency. In the top panel we show the flux $F_{\rm opt/UV}(\nu)$ corresponding to one observation taken during the main outburst. The dashed and solid lines represent the best fit to the data for $F_{\rm opt/UV} \propto \nu^{\alpha}$ (with α a free parameter) and $F_{\rm opt/UV} \propto \nu^{2}$, respectively. The results of the fit are reported in Table 4.

lower than that observed in panels "(d)" and "(e)," which is the opposite effect that one would expect.

An obvious source of systematic uncertainty is the value of $E(B-V)$ (dependent on the value of $N_{\rm H}$) which we have assumed to be constant throughout the outburst. To verify whether this is indeed affecting our results we fitted our observations with the model `reddening*diskbb` via the software *XSPEC* (v.12.8.1) by leaving $E(B-V)$ as a free parameter and fixing $N_{\rm H} = 1.4 \times 10^{21}\,{\rm cm}^{-2}$, $T_{\rm in} = 0.1$ keV and $i = 50^{\circ}$ (e.g., Patruno et al. 2009a). In this way we also take properly into account the value of reddening as a function of wavelength over the entire filter bandwidth. The first two observations have best-fits that are statistically unacceptable with null hypothesis probabilities $\ll$0.01. Changing the temperature of the diskbb model does not change the results in any significant way. The third and fourth observations are compatible with a value of $E(B-V) \simeq 0.01$–0.16, which appears to be only marginally compatible with the galactic $N_{\rm H}$ (Kalberla et al. 2005). The last two observations give a range of reddening which is unconstrained. Therefore we conclude that the data cannot be explained with a simple multicolor-disk blackbody and that there is no evidence for the data to be close to the RJ limit and therefore the low values of β need a different explanation.

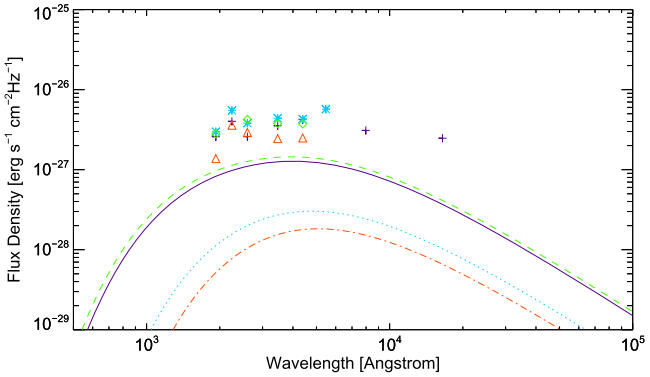

Figure 7. NIR/Optical/UV emission observed during the reflares (the symbols, with colors corresponding to different days, which are reported in Table 4) and and the predicted blackbody disk emission for the X-ray luminosity (continuous curves, with colors representing different days). Each curve corresponds to a specific $\dot{M}$ inferred from the X-ray luminosity via the relation $L_{\rm X} \simeq GM\dot{M}/R_{*}$.

Finally, we show that indeed the NIR/optical/UV emission is always larger (by a factor $\sim$10) than would be predicted assuming that the X-ray emission tracks the accretion rate so that $L_{\rm X} \simeq GM\dot{M}/R_{*}$, and that the outer disk is a standard Shakura–Sunyaev α-disk. This is seen in Figure 7, which plots the observed NIR/optical/UV flux of the 2008 outburst between MJD 54757 and 54770 and the predicted optical disk emission based on the X-ray luminosity (although note that this is based on the 2–10 keV X-ray emission, which could underpredict the bolometric luminosity by a factor of up to 3; in't Zand et al. 2007). The optical emission is brighter than would be predicted by X-rays, by a factor of a few (but it would track more closely if the X-ray bolometric flux is higher).

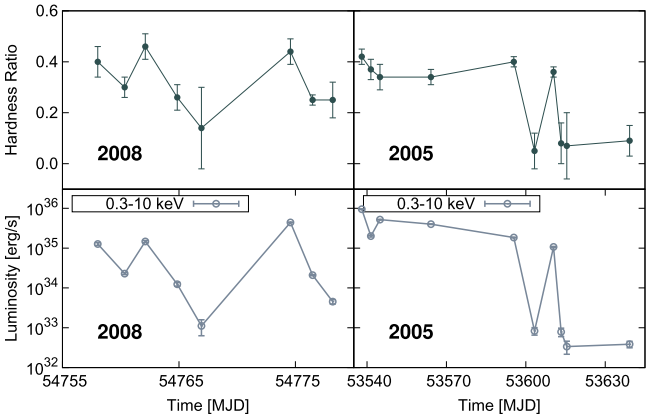

Figure 8. Hardness ratio (top panels; defined as the ratio between the count rate in the 2–10 keV and 0.3–2 keV band) of the 2008 (left panels) and 2005 (right panels) reflares. On the bottom panels we report the *Swift*/XRT light curves for comparison (we use only PC mode data and select only observations that gave useful constraints on the hardness ratio). The HR and X-ray flux are correlated in both outburst: the spectrum becomes softer at lower luminosities.

3.4. X-Ray Spectra and Colors

We have analyzed the X-ray spectra and performed a color analysis of SAX J1808.4–3658 during the 2008 and 2005 reflares (with *Swift*) to highlight any possible change in the accretion flow properties and/or geometry. In Figure 8 we show the hardness ratio results for the *Swift*/XRT observations: in both outbursts the HR shows variability which seems correlated with the variations in luminosity, i.e., the source becomes softer at lower luminosities.

Applying a standard Spearman's rank test we find an correlation coefficient of 0.93 and 0.72 (for the 2008 and 2005 outbursts respectively) but we note that the errorbars associated with the colors and luminosities are significant and unaccounted for in this method. Using a composite Monte Carlo analysis of Spearman's rank test—as detailed in Curran (2014) and implemented in the code *MCSpearman* (Curran 2014)—we find a correlation coefficient of 0.71 ± 0.21 and 0.66 ± 0.18 (for the 2008 and 2005, respectively) . This method uses a Monte Carlo re-sampling and perturbation analysis to return a robust correlation coefficient that accounts for both the uncertainty associated with the sample and the errors on individual data points. We therefore see a significant correlation between X-ray luminosity and HR, although we cannot draw any robust conclusion about the the lowest luminosities.

In our fits to the *Swift*/XRT spectra from the reflaring portion of the 2008 outburst (see Table 5) we used a spectral model consisting of some combination of a power law (`pegpwrlw`), a blackbody (`bbodyrad`), and a disk blackbody (`diskbb`), modified by photoelectric absorption. We used the `phabs` absorption model with `wilm` abundances (Wilms et al. 2000) and `vern` cross sections (Verner et al. 1996); the absorption column was in all cases fixed at a value of $N_{\rm H} = 1.4 \times 10^{21}\,{\rm cm}^{-2}$ (see Patruno et al. 2009a). For our spectral fits and count-rate conversions of the *Swift* data from the reflaring portion of the 2005 outburst we used (in all cases) a model consisting of only an absorbed power law. The disk blackbody model is required only in the two brightest observations of 2008. The choice of a disk blackbody is justified because such component is also observed during the main outburst (see e.g., Papitto et al. 2009; Patruno et al. 2009a; Kajava et al. 2011). The results of our analysis are reported in Table 5.

The power law index Γ shows little variations and all photon index values can be well fitted with a simple constant $\Gamma = 1.75 \pm 0.06$ with a $\chi^2/{\rm dof} = 6.52/7$. However, given the poor photon counts and large error bars, the behavior at the lowest luminosities remains mostly unconstrained.

We detect a blackbody with a small radius, which suggests we are observing the hot-spot or the neutrons star boundary layer rather than the thermal emission from the inner accretion disk (see also Patruno et al. 2009a; Papitto et al. 2009 for a similar analysis on *XMM-Newton* data taken during the main outburst). The two brightest reflare observations that need a multi-temperature disk blackbody (`diskbb`) still require a rather cold inner disk temperature (0.1–0.2 keV).

SAX J1808.4−3658 has remained in the hard state throughout its outburst history (from 1998 until 2011) with very little spectral variations (see e.g., van Straaten et al. 2005; Hartman et al. 2008; Bult & van der Klis 2015b). We caution that the minimum X-ray luminosity observable with *RXTE*/PCA is of the order of a few times 10^{34} erg s^{-1}.

4. DISCUSSION

In this paper we have presented a multi-wavelength analysis on the accreting millisecond pulsar SAX J1808.4−3658 that can help to address two specific (and related) issues:

1. what is the geometry of the accretion flow during reflares?
2. what is the origin of reflares and how are they affected by the presence of a magnetosphere?

4.1. Accretion Flow Geometry

To understand how the accretion flow behaves during reflares it is important to consider first whether the inner regions of the accretion flow are geometrically thin or thick and then how the flow interacts with the neutron star magnetosphere.

Since SAX J1808.4−3658 has a measured dipolar magnetic field (at the poles) of 2×10^8 G (di Salvo et al. 2008; Hartman et al. 2008), it is possible to estimate the location of its magnetospheric radius. We first define the magnetospheric radius $r_{\rm m}$ as the point where the magnetic field is strong enough to *enforce co-rotation* of gas in a thin Keplerian disk:

$$r_{\rm m} = \left(\frac{\eta\mu^2}{4\Omega_* \dot{M}}\right)^{1/5} = 2.3 \times 10^6 \eta^{1/5} \left(\frac{B_*}{10^8\,{\rm G}}\right)^{2/5} \left(\frac{R_*}{10^6\,{\rm cm}}\right)^{6/5} \times \left(\frac{P_*}{2 \times 10^{-3}\,{\rm s}}\right)^{1/5} \left(\frac{\dot{M}}{1.6 \times 10^{-10}\,M_\odot\,{\rm yr}^{-1}}\right)^{-1/5} {\rm cm}. \quad (2)$$

In this equation, $\mu = B_* R_*^3$ is the magnetic moment of the star, B_* is the neutron star magnetic field at the poles, R_* is the neutron star radius, $\eta \leqslant 1$ is a dimensionless parameter characterizing the strength of the disk/field coupling and reflects the strength of the toroidal magnetic field induced by the relative rotation between the disk and dipolar magnetic field, Ω_* (P_*) is the star's spin frequency (period) and $\dot{M}$ the mass accretion rate through the disc. If we use the known parameters of SAX J1808.4−3658 and we assume that the

Table 5
Spectral Fits to SAX J1808.4–3658 During the 2008 Reflaring State

DiskBB + BB + PL Observation	DiskBB Temp. (keV)	DiskBB Radius (km)	BB Temp. (keV)	BB Radius (km)	Γ	$L_{0.3-10\,\mathrm{keV,unabs.}}$ (10^{33} erg s^{-1})	χ^2/dof
30034041	$0.155^{+0.012}_{-0.013}$	$55.0^{+9.4}_{-7.3}$	$0.485^{+0.018}_{-0.017}$	$4.75^{+0.47}_{-0.61}$	$1.42^{+0.22}_{-0.29}$	684^{+14}_{-13}	41.2/50
30034042	$0.097^{+0.026}_{-0.023}$	130^{+166}_{-58}	$0.550^{+0.064}_{-0.052}$	$2.60^{+0.79}_{-0.58}$	$1.87^{+0.11}_{-0.16}$	490^{+14}_{-14}	55.8/51
BB + PL							
30034035	...	...	...	...	2.00 (fixed)	$0.62^{+0.38}_{-0.28}$	...
30034036	...	...	0.50(fixed)	$2.28^{+0.27}_{-0.31}$	$1.50^{+0.20}_{-0.26}$	105^{+12}_{-12}	7.9/10
30034037	...	...	$0.40^{+0.09}_{-0.06}$	$1.27^{+0.58}_{-0.41}$	$1.88^{+0.23}_{-0.24}$	20^{+16}_{-16}	10.2/14
30034038	...	...	$0.49^{+0.08}_{-0.06}$	$2.40^{+0.73}_{-0.53}$	$1.51^{+0.30}_{-0.31}$	122^{+13}_{-13}	20.3/18
30034039	...	...	0.35(fixed)	$0.62^{+0.46}_{-0.62}$	$1.89^{+0.19}_{-0.20}$	$11.7^{+1.9}_{-1.9}$	3.5/5
30034040	...	...	...	...	2.00 (fixed)	$1.1^{+0.5}_{-0.4}$	...
30034043	...	...	$0.35^{+0.03}_{-0.02}$	$1.95^{+0.34}_{-0.31}$	$1.73^{+0.14}_{-0.18}$	$18.6^{+0.9}_{-0.9}$	36.4/39
30034044	...	...	0.25(fixed)	$1.16^{+0.50}_{-1.16}$	$1.75^{+0.29}_{-0.43}$	$4.3^{+0.7}_{-0.6}$	...

observed X-ray luminosity is a good proxy for the mass accretion rate then at the lowest luminosities $r_{\rm m} \simeq 160$ km. This value[12] is significantly larger than the co-rotation radius $r_{\rm co} = 31$ km and it is even larger than the light cylinder radius $r_{\rm lc} \simeq 120$ km. The co-rotation radius is defined as that point in the disk where the Keplerian rotational velocity of the gas is equal to the rotational velocity of the magnetosphere and as soon as $r_{\rm m} > r_{\rm co}$ a centrifugal barrier sets in and matter is assumed to be ejected from the system (Illarionov & Sunyaev 1975; Romanova et al. 2004). Therefore when $r_{\rm m} > r_{\rm co}$ one cannot use Equation (2) since the $\dot{M}$ inferred from the luminosity might become a bad indicator of the mass flowing in the accretion flow (for example because of mass ejection). This means that $r_{\rm m}$ cannot be as large as 160 km, or at least, if it is, it cannot be inferred from Equation (2). If the disk were truncated outside $r_{\rm co}$ it could also be truncated outside the light cylinder $r_{\rm lc}$. In this case the magnetosphere should be devoid of matter and the radio pulsar mechanism should turn on with a strong pulsar wind preventing further accretion (see e.g., Stella et al. 1994; Burderi et al. 2001). This is what is currently thought to occur in the radio-pulsar phase of the three transitional pulsars recently discovered (Archibald et al. 2009; Papitto et al. 2013; Bassa et al. 2014; Patruno et al. 2014; Roy et al. 2014, 2015; Stappers et al. 2014) and in the quiescence phase of SAX J1808.4−3658 (Homer et al. 2001; Burderi et al. 2003; Campana et al. 2004). The fact that in SAX J1808.4−3658 the X-ray luminosity increases by three orders of magnitude right after reaching the luminosity minima on a very fast timescale of 1–2 days (see Figures 2 and 3) suggests that the radio pulsar mechanism does not turn on, although a very rapid switch cannot be excluded at the moment. Furthermore, pulsations at high luminosity (in SAX J1808.4−3658) and low luminosity (in PSR J1023+0038, Archibald et al. 2014, and XSS J12270–4859, Papitto et al. 2014) argue that accretion onto a neutron star can take place across a large range of accretion rates and therefore accretion onto the neutron star does not need to necessarily stop during the lowest luminosity phases of the reflares.

In the remainder of this paper we will assume that the radio-pulsar mechanism does not turn on during the reflares (with the aforementioned caveats) and we will consider three possible scenarios, sketched in Figure 9, to understand what happens to the accretion flow during reflares:

- **A.** The disk is truncated well beyond the co-rotation radius and a strong propeller is ejecting the majority of matter flowing in the inner regions of the disk.
- **B.** The inner disk is close to the co-rotation radius throughout the reflaring phase.
- **C.** The thin disk is truncated far away from the neutron star magnetosphere which is interacting with a geometrically thick and radiatively inefficient hot flow.

The first scenario (**A**) requires that a centrifugal barrier develops as soon as $r_{\rm m} \gtrsim r_{\rm co}$. To enter a *strong* propeller regime with matter expelled from the system, $r_{\rm m}$ needs to be larger than $r_{\rm co}$ by at least a factor $\approx$1.3 so that the gas can gain enough kinetic energy to reach the escape velocity (Spruit & Taam 1993). If a strong propeller (Illarionov & Sunyaev 1975; Romanova et al. 2005; Ustyugova et al. 2006) is operating in the system then the very-low luminosities we observe are not due to an extremely low mass flow in the disk, but instead reflect the fact that only a tiny (poorly constrained) fraction of the mass actually falls onto the neutron star surface, generating X-rays (see also Lasota et al. 1999 where a similar scenario was proposed for the dwarf nova WZ-Sge). In this case, the flow itself must likely be radiatively inefficient since otherwise the much-higher accretion rate in the disc will likely dominate the X-ray emission. In this specific case the term *radiatively inefficient* is not used to indicate the presence of a geometrically thick radiatively inefficient flow (like an advection dominated accretion flow) but it is used to describe the fact that the majority of the accretion energy is not emitted as radiation.

If $r_{\rm m}$ remains too close to $r_{\rm co}$ so that matter cannot be ejected from the system, then an accretion disk different than the

[12] The definition of $r_{\rm m}$ used in this paper is the same as in Spruit & Taam (1993) whereas the classical expression of $r_{\rm m}$ (Pringle & Rees 1972), obtained by equating the gas and magnetic pressures, gives a somewhat larger value of about 500 km, which would further strengthen the argument presented here.

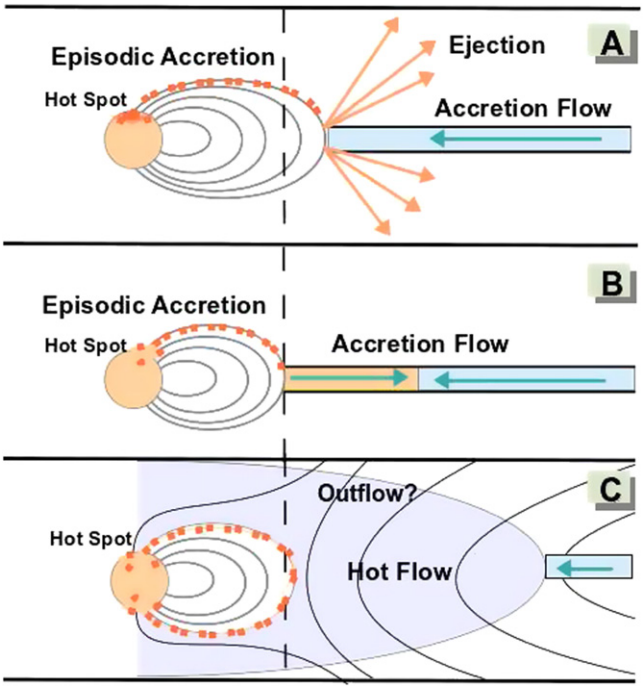

Figure 9. Different possible accretion states in SAX J1808.4−3658. The vertical dashed line refers to the co-rotation radius r_{co}. Panel A.: strong propeller configuration, when the disk is truncated well beyond r_{co} and a very large fraction of gas is expelled from the system in an outflow due to the magnetic centrifugal barrier. Episodic accretion is still expected to take place due to magnetic diffusivity, according to MHD simulations (see main text). Panel B.: trapped accretion disk scenario. The trapped disk forms when the magnetospheric radius reaches r_{co} and the disk remains truncated at that radius despite variations in the mass accretion rate. The accretion flow is modified in the inner disk regions due to the centrifugal barrier, forming a "dead disk" configuration (orange segment of the disk). The outer disk regions are unaffected by the magnetic barrier and the disk is still a standard Shakura & Sunyaev disk (light blue segment). Panel C.: truncated/radiatively inefficient accretion flow configuration. The inner disk region is set by the a mechanism other than the magnetosphere (e.g., evaporation). The resulting (geometrically thick) hot flow will still interact with the magnetosphere possibly generating accretion and/or outflows.

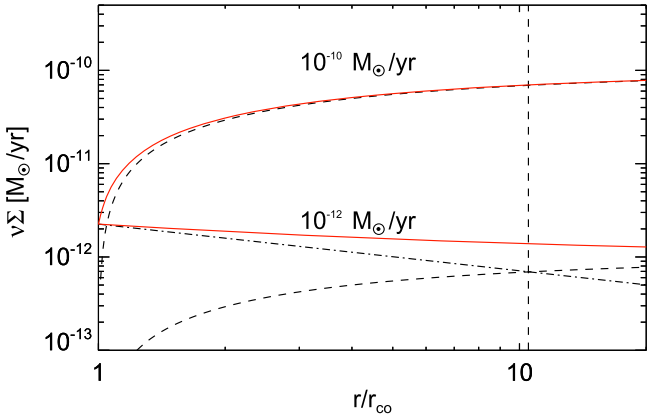

Figure 10. Surface density profile times kinetic viscosity for an accretion disk for two different mass accretion rates. The red lines are the total accretion disk density profiles, the dashed lines are two standard Shakura & Sunyaev accretion disk profiles and the dotted–dashed lines refer to a dead disk density profile. At 10^{-12} $M_\odot$ yr^{-1} the accretion disk is dominated by the dead disk solution until $r/r_{co} \approx 10$ and by the standard Shakura & Sunyaev profile beyond that point. At larger accretion rates, however, only the regions closest to the co-rotation radius are of the dead disk type and most of the accretion disk density profile is well described by a standard Shakura & Sunyaev solution.

standard geometrically thin and optically thick Shakura–Sunyaev type needs to develop (scenario **B**). Since the centrifugal barrier is not sufficient to expel the gas, the angular momentum is transferred from the magnetosphere to the matter that now remains in the inner disk regions. The gas piles up and changes the radial density and temperature profile of that region (see e.g., Figure 10). This segment of the disk is then dominated by a *trapped/dead disk* solution rather than a standard Shakura and Sunyaev one (Siuniaev & Shakura 1977). In this case the X-ray luminosity is low because only a small fraction of matter might leak from the inner (dead) disk toward the neutron star surface (D'Angelo & Spruit 2010, 2012).

Both these scenarios require that the inner accretion disk radius is set by the magnetosphere.[13] If the innermost region of the flow is not a thin disc, but instead forms a radiatively inefficient accretion flow (such as an advection dominated accretion flow, ADAF; Abramowicz et al. 1995, 2000; Narayan & Yi 1995; Narayan & McClintock 2008), then the situation might be somewhat different (scenario **C**). In most RIAF models, the accretion flow becomes optically thin but geometrically thick and somewhat sub-Keplerian (see e.g., Spruit 2000). No detailed study of the interaction between a thick disk and a magnetosphere has been undertaken, and there is considerably uncertainty about the flow geometry, location of the magnetospheric radius and propeller efficiency (e.g., Menou & McClintock 2001, Dall'Osso et al. 2014 and D'Angelo et al. 2015). In this case we expect a scenario somewhere between a thin-disk/magnetosphere interaction and quasi-spherical accretion from a stellar wind (e.g., Shakura et al. 2013), although there are many uncertainties about the properties of such a flow (e.g., the thickness of the hot flow, the inner accretion disk location, the presence of a jet and outflows; see Narayan & McClintock 2008 for a review). To assess the validity of this scenario, further investigations and theoretical modeling are required. Depending on how sub-Keplerian the RIAFs rotation is, it may also form either a trapped disk or a propeller-type outflow similar to the thin disk case. The structure of the flow (and its radiative efficiency), is strongly uncertain, and depends on the efficiency of radiative cooling from surface emission. For example, if a strong propeller forms, little radiation will come from the surface and the radiative cooling of the flow will be very inefficient (e.g., Ikhsanov 2003). On the other hand, a "hot settling flow" might form, similar to what was derived by Medvedev & Narayan (2001).

4.1.1. Observational Constraints on Accretion Flow Geometry

Having set the three different configurations for the geometry of the accretion flow and disk/magnetosphere interaction during the reflares, we now discuss how the new observations presented in this work and the past observational evidence collected from the literature can help to constrain the different scenarios. The three possibilities discussed above have a number of specific testable features that can be translated into the following questions:

[13] The region over which the disk and magnetic field interact will of course have a certain radial extent. However, both simulations and theoretical arguments predict this transition is sudden and $r_{in} = r_m$ (see e.g., Lovelace et al. 1995 and an extended discussion in D'Angelo & Spruit 2010).

1. is there a geometrically thin disk extending all the way down (or close to) the co-rotation radius? Or is the inner disk radius truncated much further away from the neutron star?
2. does the disk/magnetosphere interaction generate a strong propeller with outflows?

Constraints from X-Ray Spectral Analysis. Our spectral analysis of the reflares indicates that SAX J1808.4−3658 has an overall stable spectrum despite the large variations in luminosity. The *Swift*/XRT spectra remain hard at all luminosities and all spectra are consistent with a constant value of $\Gamma \simeq 1.7$. We do find correlated variations between the *Swift* hard color and X-ray luminosity that suggest that some (small) changes in the system are occurring in response to the X-ray luminosity variations. The *RXTE* colors further show that SAX J1808.4−3658 is observed in the hard (island and extreme island) state throughout its eight outbursts (see e.g., in't Zand et al. 1998; van Straaten et al. 2005; Hartman et al. 2008; Bult & van der Klis 2015b and Section 3.4)[14] The rather stable X-ray spectrum suggests that the production of X-rays is regulated by some stable mechanism despite large variations in the accretion flow.

During the brightest portions of the reflares we detect an accretion disk in addition to a blackbody and a power-law. A very similar spectrum was seen also during the main 2008 outburst with *XMM-Newton* (Cackett et al. 2009; Papitto et al. 2009; Patruno et al. 2009a; Kajava et al. 2011).

An important caveat is that even if the spectra of the reflares are similar to the main outburst spectra, this does not necessarily mean that the accretion flow has the same configuration. Indeed the spectra analyzed by Kajava et al. (2011) and Patruno et al. (2009a), Papitto et al. (2009) and Cackett et al. (2009) refer to luminosities about one order of magnitude brighter than the reflares.

Constraints from X-Ray Aperiodic Variability. A truncation radius close to the co-rotation one is also the preferred scenario to explain the strong 1 Hz modulation observed during the 2000, 2002 and 2005 reflares of SAX J1808.4−3658 (van der Klis 2000; Wijnands 2003; Patruno et al. 2009b). Recently, a similar modulation (1–5 Hz) has been observed also during the main outburst of the 2008 and 2011 outbursts (Bult & van der Klis 2014). In both cases an instability arising from a trapped disk (Spruit & Taam 1993; D'Angelo & Spruit 2010, 2012) has been proposed to be at the origin of this phenomenon. Such a disk model has also been discussed to explain a strikingly similar 1 Hz modulation observed in another accreting millisecond pulsar (NGC 6440 X–2; see Patruno & D'Angelo 2013). It is not possible to exclude that this variability might be related to propeller driven episodic accretion (e.g., Lii et al. 2014) which, however, needs further investigation.

A second constraints comes from the observation of the pulse amplitude of SAX J1808.4−3658 which has been recently found to depend on the upper kHz quasi-periodic oscillation (QPO) frequency (Bult & van der Klis 2015a). It has been suggested that this implies that the upper kHz QPO frequency traces the location of the inner disk region and that this region is close to the co-rotation radius throughout the outburst. This is compatible with the interpretation given for the 1 Hz QPO (Patruno et al. 2009b) and the 1–5 Hz QPO mentioned above (Bult & van der Klis 2014).

Constraints from Coherent Pulsations. Even if there are indications for the presence of a thin disk extending all the way down to the co-rotation radius, we still do not know whether we are in the presence of a propeller (**A**) or a trapped disk (**B**). Important indications can be given by the observations of coherent pulsations.

The detection of pulsations during reflares (up to the sensitivity limit of *RXTE* of about a few 10^{34} erg s^{-1}, see Patruno et al. 2009b) and the presence of a blackbody in the spectrum (down to luminosities of 10^{34} erg s^{-1}, see Table 5) does indicate that some gas keeps falling onto the neutron star surface at least during part of the reflares. Therefore accretion on the neutron star surface is not (completely) inhibited during reflares, most likely at least not down to $\sim 10^{34}$ erg s^{-1}. This is compatible with the recent findings of accretion powered pulsations in two quiescent LMXB, where pulsations are seen at X-ray luminosities of a few times 10^{33} erg s^{-1} (Archibald et al. 2014; Papitto et al. 2014), so that accretion at these luminosities is not an unprecedented occurrence. The presence of pulsations and a blackbody at low luminosities imply that—if a strong propeller is currently operating (rather than a "trapped disk")—sustained accretion onto the neutron star surface is still ongoing. Numerical MHD simulations show that during a strong propeller only a small portion of the mass flow (of the order of few percent, although the exact value *strongly* depends on the poorly constrained coupling between the magnetic field and the plasma) actually reaches the neutron star surface (e.g., via episodic accretion, Romanova et al. 2005; Ustyugova et al. 2006; Lii et al. 2014) creating a boundary layer/hot-spot that gives rise to most of the observed X-ray luminosity. Therefore if a strong propeller is currently operating in SAX J1808.4−3658 we should expect a very large mass outflow.

Such large outflow of mass might have some further observational consequences. Indeed if the amount of material reaching the surface is truly only a very small fraction of the total amount of matter flung off the disk, then we should still expect a rather strong spin down of the neutron star. So far, SAX J1808.4−3658 has not been observed to spin up or down during its outbursts, with typical upper limits of $|\dot{\nu}| \lesssim 2.5 \times 10^{-14}$ Hz s^{-1} (Hartman et al. 2008, 2009; Patruno et al. 2012), a fact that again suggests that this object does indeed stay close to spin equilibrium ($r_{\rm m} \simeq r_{\rm co}$) during most of its outbursts (see also e.g., Haskell & Patruno 2011). Although these upper limits refer to the entire outburst and not only to the reflaring portion, we note that at least in one case (the 2000 outburst) *RXTE* collected data exclusively during the reflares (due to solar constraints). In that case the upper limits on the spin frequency derivative were even more stringent: -1.1×10^{-14} Hz s^{-1} $\leqslant \dot{\nu} \leqslant 4.4 \times 10^{-14}$ Hz s^{-1} (95% confidence interval, see Table 4 in Hartman et al. 2008).

Episodic accretion might possibly have a role to explain why we do not see a strong spin down despite the strong propeller since the angular momentum loss due to the centrifugal barrier might be (partially) compensated by the material torque accreting onto the neutron star surface. However, to determine the order of magnitude expected we can use the relation:

$$\begin{aligned} \dot{J}_{\rm prop} &= -\, n\dot{M}_{\rm ej}\left(GMr_{\rm in}\right)^{1/2} \\ &= -\, n\left(r_{\rm in}/r_{\rm co}\right)^{1/2}\dot{M}_{\rm ej}\left(GMr_{\rm co}\right)^{1/2}, \end{aligned} \quad (3)$$

[14] An exception is represented by the highest X-ray luminosities reached at the peak of the outburst, when the source briefly (1–2 days) moves to the lower-left banana branch and the lower kHz QPO appears (Bult & van der Klis 2015b).

where r_{in} is the inner disk radius and the dimensionless torque n is zero for $r_{in} = r_{co}$ and of order unity for $r_{in} \gtrsim 1.1\ r_{co}$ (Ekşi et al. 2005). For $r_{in} \approx$ 1–2 r_{co} and $\dot{M}_{ej} \approx 10^{-10}\ M_{\odot}\ \mathrm{yr}^{-1}$ we obtain a spin down of the order of a few times 10^{-14} Hz s^{-1}. Such values are of the same order of magnitude as the upper limits placed in most of the outbursts (see e.g., Hartman et al. 2009 and Table 4 in Hartman et al. 2008). The choice of $\dot{M}_{ej} \approx 10^{-10}\ M_{\odot}\ \mathrm{yr}^{-1}$ derives from the fact that this is the approximate value required to produce X-ray luminosities of a few times 10^{35} erg s^{-1}, which is the typical value observed at the peak of the reflares. Since the material falling on the neutron star has to be at least $10^{-10}\ M_{\odot}\ \mathrm{yr}^{-1}$, then the expected spin-down above is the minimum that we can expect in this scenario. The constraints on the observations (at least for the 2000 reflares) suggest that any spin down present in SAX J1808.4−3658 must be smaller than this minimal expected $\dot{\nu}$ value. However, given the uncertainties in the model and the close value between the expected $\dot{\nu}$ and the observed upper limits, this result should be taken more as a possible indication against the strong propeller rather than conclusive evidence.

The lack of a detected spin-down can also be important to place constraints on the trapped disk scenario (**B**). The sign of the torque depends on whether the inner edge of the disk is inside or outside the co-rotation region, and the amplitude is roughly determined by the "critical accretion rate"–$\dot{M}_c$, the accretion rate at which the inner edge of the disk is equal to the co-rotation radius. In D'Angelo & Spruit (2012) this was estimated as:

$$\dot{M}_c = \frac{\eta\mu^2}{4\Omega_* {r_c}^5}, \tag{4}$$

and corresponds to $\dot{M}_c \sim 5 \times 10^{-11} M_{\odot}\ \mathrm{yr}^{-1}$ for SAX J1808.4−3658 (assuming a magnetic field of 10^8 G). The amplitude of the spin-up/spin-down torque is then roughly:

$$\dot{J}_c = \dot{M}_c \left(GM_* r_c\right)^{1/2} \tag{5}$$

which (assuming a moment of inertia of 10^{45} g cm^2) corresponds to a spin change of $\Delta\nu \sim 10^{-14}$ Hz. For a mean outburst accretion rate of $\dot{M} \sim 2 \times 10^{-10} M_{\odot}\ \mathrm{yr}^{-1}$ this corresponds to a spin up rate of $\sim$(0.3–1) $\times\ 10^{-13}$ Hz s^{-1}. For the long-term average accretion rate of $\dot{M} \sim 5 \times 10^{-12}\ M_{\odot}\ \mathrm{yr}^{-1}$ (i.e., averaged over an entire outburst/quiescence cycle), the spin-up from accretion is nearly balanced by spin-down from the disk–magnetosphere coupling outside r_c, and more detailed calculations predict a net spin down rate of (1–3) $\times\ 10^{-14}$ Hz s^{-1} (see also Figure 2 of D'Angelo & Spruit 2012). Such values are not much different than those obtained for the propeller scenario (**A**) and indeed similar conclusions can be drawn: the expected spin up/down from a trapped disk is too close to the existing measured upper limits to place robust constraints on the operating mechanism.

Finally, it is worth noticing that the lack of a spin-down during the outbursts might still be compatible with the scenario **C**, where a thick hot flow is present up to a very large distance from the neutron star. In this case it might be the sub-Keplerian nature of the hot flow itself that results in a very small amount of angular momentum transferred toward the neutron star and thus in a lack of detected accretion torques. In Table 6 we summarize which of the observed properties can be explained by each of the models considered here.

4.2. The Origin of Reflares

Reflares are an important phenomenon to study because they are assumed to be generated by the ionization instability that drives dwarf novae and X-ray binary outbursts. Therefore understanding why reflares are sometimes observed can give important information about how the ionization instability operates. Even more importantly, their observation can help testing the assumption that they are indeed generated by the ionization instability.

Reflares are currently considered a problem for the disk instability model since they require that a large amount of matter is retained in the disk a the end of the main outburst (Dubus et al. 2001; Arai et al. 2009). The currently best explanation (which qualitatively agrees with the observed timescales and luminosity fluctuations) is that reflares are essentially "mini-outbursts." A small change in disk density at the end of an outburst increases the outer disk temperature enough to partially ionize hydrogen, which then leads to a rapid rise in the accretion rate into the inner disk and a rebrightening. The exact trigger of the reflare is uncertain—they appear spontaneously in the simulations of Dubus et al. (2001), although they do not resemble the observed reflares and they are seen by Hameury et al. (2000) where reflares are caused by an increased irradiation of the donor star that causes a superoutburst (so called because their duration is much larger than that of normal outbursts) followed by reflares. The donor star in SAX J1808.4−3658 is observed to be strongly irradiated during quiescence (Homer et al. 2001; Burderi et al. 2003; Campana et al. 2004) and indeed there are suggestions that it is losing a large amount of mass (di Salvo et al. 2008; see however Patruno et al. 2012 and Hartman et al. 2008 for criticisms of this strong mass loss scenario in SAX J1808.4−3658). Another suggestion for the reflare trigger comes from the mass reservoir model of Osaki et al. (2001), where reflares are triggered also after superoutbursts as long as the effective viscosity of the disk (parametrized by the α parameter) remains large through the entire sequence of reflares.

So far little work has been done on reflares occurring in X-ray binaries and most theoretical work has focused on explain the reflaring phenomenon observed in the dwarf novae population (see however, Augusteijn et al. 1993; Chen et al. 1993; Kuulkers 1998 for reflares occurring in black hole binaries). However, regardless of the trigger (which might be of a different nature than outlined above), the reflares should proceed in the same way: at the end of an outburst the temperature at some location in the outer disk falls below the hydrogen ionization temperature, causing hydrogen to recombine and the accretion rate to fall dramatically as a "cooling wave" travels inward. For (possibly) one of the reasons outlined by the irradiation or mass reservoir model, the density in the disk subsequently rises again enough to reach the hydrogen ionization temperature and again send a new "heating" wave through the disk, which causes the accretion rate to rise. Since there is not a large amount of gas left in the accretion disk after the main outburst, the accretion rate again decreases, resetting the entire process.

In WZ-Sge type systems, the reflares are observed after the occurrence of a superoutburst, so called because its duration is much larger than that of normal outbursts. In these systems, it

Table 6
Models for the Geometric Configuration of the Accretion Flow

Model	X-Ray Spectra	Spin-down	1 Hz QPO	Weak Irradiation	X-Ray Delay	NIR/Optical/UV Excess
Strong Propeller (**A.**)	P	P	P	?	Y	Y
Trapped/Dead Disk (**B.**)	Y	P	P	?	Y	Y
Thick Hot Flow (**C.**)	N	P	N	?	Y	Y

Note. The table compares observed properties of the to the various models discussed in Section 4. Y/N (yes/no) indicates that the model can/cannot explain the property in SAX J1808.4−3658. The symbol P (possible) indicates that the model might be able to explain the property if certain conditions are met. The symbol ? indicates that the model makes no specific prediction for that property, and that further studies are required.

was proposed that a resonance occurs when the disk radius exceeds the threshold of $0.46a$ where a is the orbital semi-major axis. When this happens superhumps are expected to develop (Osaki 1989, 1996). Black hole candidates in X-ray binaries displaying superhumps do not show outbursts of varied amplitudes (Maccarone 2014) and SAX J1808.4−3658 does follow the same behavior. It is possible that both SAX J1808.4−3658 and those black hole candidates have shown only superoutbursts. Maccarone & Patruno (2013) suggested indeed that we do observe only super-outbursts from some LMXBs and superhumps should be detected if the reflares in SAX J1808.4−3658 are a variant of those seen in dwarf novae.

Elebert et al. (2009) reported weak evidence for the presence of a superhump at optical wavelengths in SAX J1808.4–3658, which, if confirmed, might be an exciting observational diagnostic and might indicate the presence of an eccentric disk. However, the candidate superhump has been observed so far only once during the main 2008 outburst and it attends further confirmation.

Regardless of the presence of superoutbursts, this basic hot/cold wave scenario can plausibly account for the reflares in SAX J1808.4–3658. If the instability originates in the outer part of the disk, the reflare rise time can be associated with the time it takes for the heating front to propagate from the outer edge of the disk to the central regions, which will happen on a thermal timescale:

$$t_{\rm r} \sim r_{\rm d}/\alpha c_{\rm s} \quad (6)$$

where $r_{\rm d}$ is the location of the outer edge of the disk, $\alpha = 0.1$ is the Shakura–Sunyaev viscosity parameter, and $c_{\rm s}$ is the sound speed at the inner edge of the heating front, where $T \sim 6500$ K. For a 2-day rise time, $r_{\rm d} \sim 10^{10}$ cm, which is comparable to the circularization radius of the disk $r_{\rm cr} \sim 0.46a \sim 3 \times 10^{10}$ cm (assumed to be the outer disk edge; a is the projected semi-major axis of the binary, for the orbital period 7249 s and assumed NS mass of $1.4 M_{\odot}$ and donor companion of $0.07\ M_{\odot}$).

4.2.1. Constraints from Multiwavelength Photometry

During the reflaring phase of the 2008 (and to some extent also 2005) outburst, we can place three constraints on the nature of the accretion disk in SAX J1808.4−3658. The first constraint comes form the observation of *weak* irradiation as witnessed by the small value of β (see Section 3.2). This usually suggests that the accretion disk is heated mostly by viscous dissipation rather than irradiation (see e.g., Russell et al. 2006). The reason why irradiation is not the main contributor to the optical/UV flux emission remains an open question.

The second constraint comes from the observation of some anti-correlations between X-ray and optical/NIR emission (e.g., Figure 2 on MJD 54746–54747 and MJD 54758 and several data point in Figure 3). As discussed in Section 3.1 there is a tentative X-ray delay of about 1.5 days with respect to the NIR/optical emission.[15] The X-ray delay is a phenomenon that has been already observed in other LMXBs although so far only in systems containing black holes. In some systems (two of which are persistent sources) the optical/X-ray cross-correlations shows evidence for X-ray delays on the order of ∼5–20 days. Brocksopp et al. (2001) found an X-ray lag of 5–10 days from long-term optical and X-ray light-curves of the black hole binary LMC X–3 (a persistent source; see also Steiner et al. 2014 who measured this delay as 2 weeks). Homan et al. (2005) found an X-ray lag of 15–20 days compared to near-IR variations in the black hole LMXB GX 339–4 (a transient source). An X-ray lag of 2–14 days was observed in 4U 1957+11 (persistent) behind optical (Russell et al. 2010), whereas a 3.5 d X-ray time lag compared to UV was found in Swift J1910.2–0546 (a transient source; Nakahira et al. 2014). Such delays have been interpreted with a variety of models that propose that the NIR/optical/UV emission originates from a jet, from the outer disk or even from the irradiated stellar surface.

In the case of SAX J1808.4−3658 we do not have sufficient observational evidence to constrain the presence of a jet during the reflares. Since the jet model (or an ADAF with an outflow) cannot be constrained we will not consider it any further, although we stress that there is still no proof that can firmly exclude such scenario.

If we consider a disk origin of the emission then we can assume that the NIR/optical/UV emission is coming from the outermost disk regions. In this case by looking at Figure 7 it is clear that this emission is over-luminous with respect to the X-rays luminosity. It is possible that, when the heating front moves inward and reaches the inner disk regions, a larger flow of X-rays is produced which would correspond to the peak of the reflares. However, the peaks are still too dim for the optical luminosity observed and therefore this scenario is unable to explain the observed behavior.

On the other hand, if an outflow is present and a significant portion of mass is lost from the system then a strongly over-luminous NIR/optical/UV emission is expected. Indeed if the material generating radiation is lost in the disk before reaching the innermost regions then the X-rays will not be produced. In other words this means that the X-ray luminosity is not a good tracer of the mass accretion rate. This is a phenomenon that has been already independently suggested to explain the behavior of the upper kHz QPO in relation of the pulse amplitude in SAX J1808.4−3658 (Bult & van der Klis 2015a) and the

[15] We also note that during *some observations* of the 2000 outburst (see Wachter et al. 2000; Wijnands 2006) the optical luminosity also did not correlate with the X-ray luminosity.

parallel track phenomenon in LMXBs (van der Klis 2001). The over-luminous NIR/optical/UV emission can explain the possible X-ray delay, as well as our third important constraint: any multicolor-disk model of a viscously heated accretion disk seems to modestly under-predict the optical luminosity observed for the measured X-ray luminosity (see Section 3.3). Since the optical emission is only over-predicted by a factor of a few with respect to the X-ray flux (assuming a constant accretion rate through the disk) our results also exclude a very strong outflow in the disk. Such an outflow would expel the majority of gas before it radiated energy in X-rays, which would make the discrepancy between optical and X-rays much larger. However, it is still possible that some (not too strong) outflow of material is present in the system, which could be driven either by a magnetospheric RIAF (like the strong propeller; Ustyugova et al. 2006) or by an accretion driven RIAF (like a wind; Blandford & Begelman 1999), is present in the system.

Finally, almost identical conclusions can be reached for the scenario **B** (trapped disk). In Figure 10 we compare the surface density profiles (times the kinetic viscosity) of a standard accretion disk and a trapped/dead disk. The extent of the trapped disk region could be modest which means that the largest majority of the accretion disk would still look and behave as a standard Shakura & Sunyaev accretion disk. This means that at large accretion rates the total disk profile would be observationally indistinguishable (in luminosity and spectral properties) from a Shakura & Sunyaev disk, despite the presence of a small segment where the dead disk is still present. Therefore identical considerations discussed above apply to this scenario too. We caution that the extent of the region where the dead disk dominates strongly depends on the efficiency of the angular momentum extraction at the inner edge of the disk, a quantity that is currently poorly known.

Interpreting the reflares in terms of a specific physical model is hampered by the uncertain origin of the UV/optical/NIR emission. Assuming that it is dominated by a single physical component, the simplest explanation would be that it originates in the outer parts of the accretion disk, either directly from viscous dissipation or as reprocessed emission from irradiation from the inner X-ray component. However, as discussed in 3.3 and 4.1.1, we consider it unlikely to be reprocessed emission and its origin remains still to be identified.

5. CONCLUSIONS

In this paper we have analyzed the 2008 and 2005 reflaring phase of the accreting millisecond pulsar SAX J1808.4−3658. We find that the accretion flow geometry can be substantially constrained by the occurrence of reflares. We find that a disk extending down to the co-rotation radius and truncated by the neutron star magnetosphere provides the most likely explanation for the accretion flow. We have found that the NIR/optical/UV emission during the reflares is over-luminous and cannot be explained by an irradiated accretion disk model if the mass accretion rate used is inferred from the observed X-ray luminosity. We suggest that most of the NIR/optical/UV emission comes from the outer disk and it is produced by viscous dissipation. The mass accretion rate in the outer disk regions needs to be substantially higher than the one that reaches the inner disk regions. We propose that either a propeller with a large amount of matter being expelled from the system or a trapped (dead) disk truncated at the co-rotation radius are both plausible explanations for all of these features. A disk truncated (by e.g., evaporation) far away from the neutron stars (at hundreds or even thousands gravitational radii) is instead not supported by the current observational evidence. Finally, we find that a hot/cold wave propagation model for the reflarings is compatible with the observed timescales although the mechanism that triggers such phenomenon is still to be identified.

We would like to thank Jari Kajava, Erik Kuulkers and Peter Bult for interesting discussions and suggestions. A.P. acknowledge support from a Netherlands Organization for Scientific Research (NWO) Vidi Fellowship. This work was partially supported by Australian Research Council grant DP120102393. This research has made use of data obtained by the CTIO 1.3 m telescope operated by the *SMARTS* consortium. This work made use of data supplied by the UK Swift Science Data Centre at the University of Leicester.

REFERENCES

Abramowicz, M. A., Chen, X., & Taam, R. E. 1995, ApJ, 452, 379
Abramowicz, M. A., Lasota, J.-P., & Igumenshchev, I. V. 2000, MNRAS, 314, 775
Allen, J. L., Linares, M., Homan, J., & Chakrabarty, D. 2015, ApJ, 801, 10
Arai, A., Uemura, M., Sasada, M., et al. 2009, in ASP Conf. Ser. 404, The Eighth Pacific Rim Conference on Stellar Astrophysics: A Tribute to Kam-Ching Leung, ed. S. J. Murphy & M. S. Bessell (San Francisco, CA: ASP), 87
Archibald, A. M., Bogdanov, S., Patruno, A., et al. 2015, ApJ, 807, 62
Archibald, A. M., Stairs, I. H., Ransom, S. M., et al. 2009, Sci, 324, 1411
Armas Padilla, M., Degenaar, N., Russell, D. M., & Wijnands, R. 2013, MNRAS, 428, 3083
Augusteijn, T., Kuulkers, E., & Shaham, J. 1993, A&A, 279, L13
Bailyn, C. D., & Orosz, J. A. 1995, ApJL, 440, L73
Bassa, C. G., Patruno, A., Hessels, J. W. T., et al. 2014, MNRAS, 441, 1825
Bayless, A. J., Robinson, E. L., Hynes, R. I., Ashcraft, T. A., & Cornell, M. E. 2010, ApJ, 709, 251
Bessell, M. S., Castelli, F., & Plez, B. 1998, A&A, 333, 231
Bildsten, L., & Chakrabarty, D. 2001, ApJ, 557, 292
Blandford, R. D., & Begelman, M. C. 1999, MNRAS, 303, L1
Brocksopp, C., Groot, P. J., & Wilms, J. 2001, MNRAS, 328, 139
Bult, P., & van der Klis, M. 2014, ApJ, 789, 99
Bult, P., & van der Klis, M. 2015a, ApJL, 798, L29
Bult, P., & van der Klis, M. 2015b, ApJ, 806, 90
Burderi, L., Di Salvo, T., D'Antona, F., Robba, N. R., & Testa, V. 2003, A&A, 404, L43
Burderi, L., Possenti, A., D'Antona, F., et al. 2001, ApJL, 560, L71
Burrows, D. N., Hill, J. E., Nousek, J. A., et al. 2005, SSRv, 120, 165
Buxton, M. M., Bailyn, C. D., Capelo, H. L., et al. 2012, AJ, 143, 130
Cackett, E. M., Altamirano, D., Patruno, A., et al. 2009, ApJL, 694, L21
Campana, S., D'Avanzo, P., Casares, J., et al. 2004, ApJL, 614, L49
Campana, S., & Stella, L. 2004, NuPhS, 132, 427
Campana, S., Stella, L., & Kennea, J. A. 2008, ApJL, 684, L99
Chakrabarty, D., & Morgan, E. H. 1998, Natur, 394, 346
Chen, W., Livio, M., & Gehrels, N. 1993, ApJL, 408, L5
Curran, P. A. 2014, arXiv:1411.3816
Dall'Osso, S., Perna, R., & Stella, L. 2015, MNRAS, 449, 2144
D'Angelo, C. R., Fridriksson, J. K., Messenger, C., & Patruno, A. 2015, MNRAS, 449, 2803
D'Angelo, C. R., & Spruit, H. C. 2010, MNRAS, 406, 1208
D'Angelo, C. R., & Spruit, H. C. 2012, MNRAS, 420, 416
Deloye, C. J., Heinke, C. O., Taam, R. E., & Jonker, P. G. 2008, MNRAS, 391, 1619
Di Salvo, T., & Burderi, L. 2003, A&A, 397, 723
di Salvo, T., Burderi, L., Riggio, A., Papitto, A., & Menna, M. T. 2008, MNRAS, 389, 1851
Dubus, G., Hameury, J.-M., & Lasota, J.-P. 2001, A&A, 373, 251
Ekşi, K. Y., Hernquist, L., & Narayan, R. 2005, ApJL, 623, L41
Elebert, P., Reynolds, M. T., Callanan, P. J., et al. 2009, MNRAS, 395, 884
Elias, J. H., Frogel, J. A., Matthews, K., & Neugebauer, G. 1982, AJ, 87, 1029
Evans, P. A., Beardmore, A. P., Page, K. L., et al. 2007, A&A, 469, 379

Evans, P. A., Beardmore, A. P., Page, K. L., et al. 2009, MNRAS, 397, 1177
Evans, P. A., Osborne, J. P., Beardmore, A. P., et al. 2014, ApJS, 210, 8
Frogel, J. A., Persson, S. E., Matthews, K., & Aaronson, M. 1978, ApJ, 220, 75
Galloway, D. K., & Cumming, A. 2006, ApJ, 652, 559
Greenhill, J. G., Giles, A. B., & Coutures, C. 2006, MNRAS, 370, 1303
Güver, T., & Özel, F. 2009, MNRAS, 400, 2050
Hameury, J.-M., Lasota, J.-P., & Warner, B. 2000, A&A, 353, 244
Hartman, J. M., Patruno, A., Chakrabarty, D., et al. 2008, ApJ, 675, 1468
Hartman, J. M., Patruno, A., Chakrabarty, D., et al. 2009, ApJ, 702, 1673
Haskell, B., & Patruno, A. 2011, ApJL, 738, L14
Heinke, C. O., Jonker, P. G., Wijnands, R., Deloye, C. J., & Taam, R. E. 2009, ApJ, 691, 1035
Heinke, C. O., Jonker, P. G., Wijnands, R., & Taam, R. E. 2007, ApJ, 660, 1424
Homan, J., Buxton, M., Markoff, S., et al. 2005, ApJ, 624, 295
Homer, L., Charles, P. A., Chakrabarty, D., & van Zyl, L. 2001, MNRAS, 325, 1471
Howell, S. B., De Young, J., Mattei, J. A., et al. 1996, AJ, 111, 2367
Hynes, R. I., & Haswell, C. A. 1999, MNRAS, 303, 101
Hynes, R. I., Haswell, C. A., Shrader, C. R., et al. 1998, MNRAS, 300, 64
Hynes, R. I., Horne, K., O'Brien, K., et al. 2006, ApJ, 648, 1156
Ikhsanov, N. R. 2003, A&A, 399, 1147
Illarionov, A. F., & Sunyaev, R. A. 1975, A&A, 39, 185
in't Zand, J. J. M., Heise, J., Muller, J. M., et al. 1998, A&A, 331, L25
in't Zand, J. J. M., Jonker, P. G., & Markwardt, C. B. 2007, A&A, 465, 953
Jahoda, K., Markwardt, C. B., Radeva, Y., et al. 2006, ApJS, 163, 401
Kajava, J. J. E., Ibragimov, A., Annala, M., Patruno, A., & Poutanen, J. 2011, MNRAS, 417, 1454
Kalberla, P. M. W., Burton, W. B., Hartmann, D., et al. 2005, A&A, 440, 775
Kotko, I., Lasota, J.-P., Dubus, G., & Hameury, J.-M. 2012, A&A, 544, A13
Kuulkers, E. 1998, NewAR, 42, 1
Kuulkers, E., Howell, S. B., & van Paradijs, J. 1996, ApJL, 462, L87
Lasota, J.-P. 2001, NewAR, 45, 449
Lasota, J.-P., Kuulkers, E., & Charles, P. 1999, MNRAS, 305, 473
Lewis, F., Russell, D. M., Jonker, P. G., et al. 2010, A&A, 517, A72
Li, F. K., Sprott, G. F., & Clark, G. W. 1976, ApJ, 203, 187
Lii, P. S., Romanova, M. M., Ustyugova, G. V., Koldoba, A. V., & Lovelace, R. V. E. 2014, MNRAS, 441, 86
Lovelace, R. V. E., Romanova, M. M., & Bisnovatyi-Kogan, G. S. 1995, MNRAS, 275, 244
Maccarone, T. J. 2014, SSRv, 183, 101
Maccarone, T. J., & Patruno, A. 2013, MNRAS, 428, 1335
Maitra, D., & Bailyn, C. D. 2008, ApJ, 688, 537
Medvedev, M. V., & Narayan, R. 2001, ApJ, 554, 1255
Menou, K., Hameury, J.-M., Lasota, J.-P., & Narayan, R. 2000, MNRAS, 314, 498
Menou, K., & McClintock, J. E. 2001, ApJ, 557, 304
Nakahira, S., Negoro, H., Shidatsu, M., et al. 2014, PASJ, 66, 84
Narayan, R., & McClintock, J. E. 2008, NewAR, 51, 733
Narayan, R., & Yi, I. 1995, ApJ, 452, 710
Osaki, Y. 1989, PASJ, 41, 1005
Osaki, Y. 1996, PASP, 108, 39
Osaki, Y., Meyer, F., & Meyer-Hofmeister, E. 2001, A&A, 370, 488
Papitto, A., de Martino, D., Belloni, T. M., et al. 2015, MNRAS, 449, L26
Papitto, A., di Salvo, T., D'Aı, A., et al. 2009, A&A, 493, L39
Papitto, A., Ferrigno, C., Bozzo, E., et al. 2013, Natur, 501, 517
Patruno, A., Archibald, A. M., Hessels, J. W. T., et al. 2014, ApJL, 781, L3
Patruno, A., Bult, P., Gopakumar, A., et al. 2012, ApJL, 746, L27
Patruno, A., & D'Angelo, C. 2013, ApJ, 771, 94
Patruno, A., Rea, N., Altamirano, D., et al. 2009a, MNRAS, 396, L51
Patruno, A., Watts, A., Klein Wolt, M., Wijnands, R., & van der Klis, M. 2009b, ApJ, 707, 1296
Patruno, A., & Watts, A. L. 2012, arXiv:1206.2727
Patterson, J., Masi, G., Richmond, M. W., et al. 2002, PASP, 114, 721
Patterson, J., Uthas, H., Kemp, J., et al. 2013, MNRAS, 434, 1902
Pei, Y. C. 1992, ApJ, 395, 130
Poole, T. S., Breeveld, A. A., Page, M. J., et al. 2008, MNRAS, 383, 627
Pringle, J. E., & Rees, M. J. 1972, A&A, 21, 1
Psaltis, D., & Chakrabarty, D. 1999, ApJ, 521, 332
Revnivtsev, M. G. 2003, AstL, 29, 383
Robertson, J. W., Honeycutt, R. K., & Turner, G. W. 1995, PASP, 107, 443
Romanova, M. M., Ustyugova, G. V., Koldoba, A. V., & Lovelace, R. V. E. 2004, ApJ, 610, 920
Romanova, M. M., Ustyugova, G. V., Koldoba, A. V., & Lovelace, R. V. E. 2005, ApJL, 635, L165
Roming, P. W. A., Kennedy, T. E., Mason, K. O., et al. 2005, SSRv, 120, 95
Roy, J., Bhattacharyya, B., & Ray, P. S. 2014, ATel, 5890, 1
Roy, J., Ray, P. S., Bhattacharyya, B., et al. 2015, ApJL, 800, L12
Russell, D. M., Fender, R. P., Hynes, R. I., et al. 2006, MNRAS, 371, 1334
Russell, D. M., Fender, R. P., & Jonker, P. G. 2007, MNRAS, 379, 1108
Russell, D. M., Lewis, F., Roche, P., et al. 2010, MNRAS, 402, 2671
Shakura, N. I., Postnov, K. A., Kochetkova, A. Y., & Hjalmarsdotter, L. 2013, PhyU, 56, 321
Šimon, V. 2010, A&A, 513, A71
Siuniaev, R. A., & Shakura, N. I. 1977, PAZh, 3, 262
Smak, J. 1984, PASP, 96, 5
Spruit, H. C. 2000, arXiv:astro-ph/0003143
Spruit, H. C., & Taam, R. E. 1993, ApJ, 402, 593
Stappers, B. W., Archibald, A. M., Hessels, J. W. T., et al. 2014, ApJ, 790, 39
Steiner, J. F., McClintock, J. E., Orosz, J. A., et al. 2014, ApJ, 783, 101
Stella, L., Campana, S., Colpi, M., Mereghetti, S., & Tavani, M. 1994, ApJL, 423, L47
Subasavage, J. P., Bailyn, C. D., Smith, R. C., et al. 2010, Proc. SPIE, 7737, 1
Tomsick, J. A., Kalemci, E., & Kaaret, P. 2004, ApJ, 601, 439
Ustyugova, G. V., Koldoba, A. V., Romanova, M. M., & Lovelace, R. V. E. 2006, ApJ, 646, 304
van der Horst, A. J., Curran, P. A., Miller-Jones, J. C. A., et al. 2013, MNRAS, 436, 2625
van der Klis, M. 2000, ARA&A, 38, 717
van der Klis, M. 2001, ApJ, 561, 943
van Straaten, S., van der Klis, M., & Wijnands, R. 2005, ApJ, 619, 455
Verner, D. A., Ferland, G. J., Korista, K. T., & Yakovlev, D. G. 1996, ApJ, 465, 487
Wachter, S., Hoard, D. W., Bailyn, C., et al. 2000, BAAS, 32, 1219
Wang, Z., Bassa, C., Cumming, A., & Kaspi, V. M. 2009, ApJ, 694, 1115
Wijnands, R. 2003, ApJ, 588, 425
Wijnands, R. 2006, in Trends in Pulsar Research, ed. J. A. Lowry (New York: Nova Science Publishers), 53
Wijnands, R., Méndez, M., Markwardt, C., et al. 2001, ApJ, 560, 892
Wijnands, R., & van der Klis, M. 1998, Natur, 394, 344
Wilms, J., Allen, A., & McCray, R. 2000, ApJ, 542, 914
Zurita, C., Sánchez-Fernández, C., Casares, J., et al. 2002, MNRAS, 334, 999